Fig. 5. Hourly beach photography indicating a persistent shoreline projection north of traverse.

Fig. 6. Sand waves revealed by aerial photography on the Caspian Sea coast (Kobets, 1958).

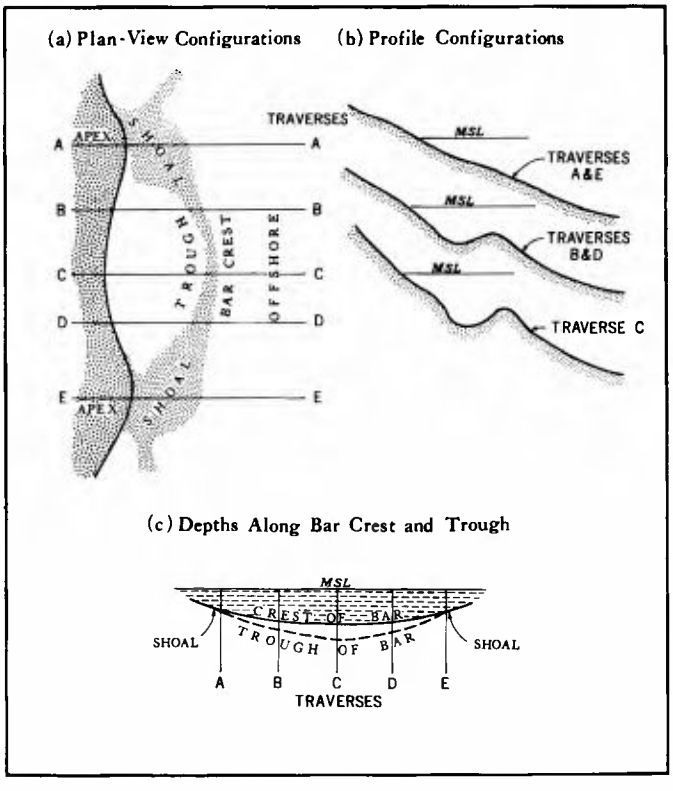

Fig. 7.

Idealized schematic of coastal sand wave (adapted from Hom-ma and Sonu, 1962).

for about a month. The strongest north flowing current, which occurred in the middle of April, was followed by a fill that was distinctly ahead of the average seasonal trend Still more significant, the three strongest south flowing currents correspond with the largest cuts along the pier.'

Characteristics of coastal sand waves have been described by Hom-ma and Sonu (1962), Krumbein and Oshiek (1950), Evans (1939), Kashechkin and Uglev, Bruun (1954), Sonu (1961,1964), Taney (1963), and Sitarz (1963). The sand waves develop when longshore currents are present. The basic geometry consists of elongate ridges and troughs oriented at angles to the shore (Figure 6). Figure 7 shows schematically sand-wave nearshore topography. The shoreline embayment is associated with a wave trough and the projection a wave crest, without an offshore bar.

The migration of sand-wave topography also has been reported. Egorov (1951a) noted from 15 to 32 m migration in 24 hours. Bruun (1954) reported an average annual displacement of 1,000 m. Mogi (1960) and Hom-ma and Sonu (1962) found short-term fluctuations, yet no net long-term migration, on an unobstructed beach. Similar conditions were found on the Outer Banks near an observational pier. Just to the north is a persistent projection that appears in hourly photographs taken for more than 6 months (Figure 5). As shown in Figure 8 the winds arrived mainly from northeast or southeast quadrants, as did waves. Thus short-term fluctuations may have balanced each other, leaving a zero balance over the long term.

TRANSVERSAL VERSUS ALONGSHORE RESPONSES

The following analysis is based on 64 profiles, each with 37 stations 20 feet apart (Figure 2-A). Figure 2-B shows the mean profile for all the observations. The observed sequence in profile configuration is shown by the envelopes in Figure 9. It was found that by introducing an alternative measure, instead of true water depth, basic configurations in individual profiles could be discriminated. The measure used is the deviation of individual water depths from the mean depth at corresponding stations on other profiles, viz.,

$$D'_{i,j} = D_{i,j} - \bar{D}_i$$

where $D_{i,j}$ denotes the true water depth at the i-th station of the j-th profile, $\bar{D}_i$ the mean of all the depth readings made at the same i-th station, and $D'_{i,j}$ the alternative measure. Figure 10 is the time history of the surf-zone profiles using this alternative measure, shown also by the envelopes.

Out of the 64 profiles, only 7 different profile configurations can be discriminated. This suggests that two differing types of topographic response

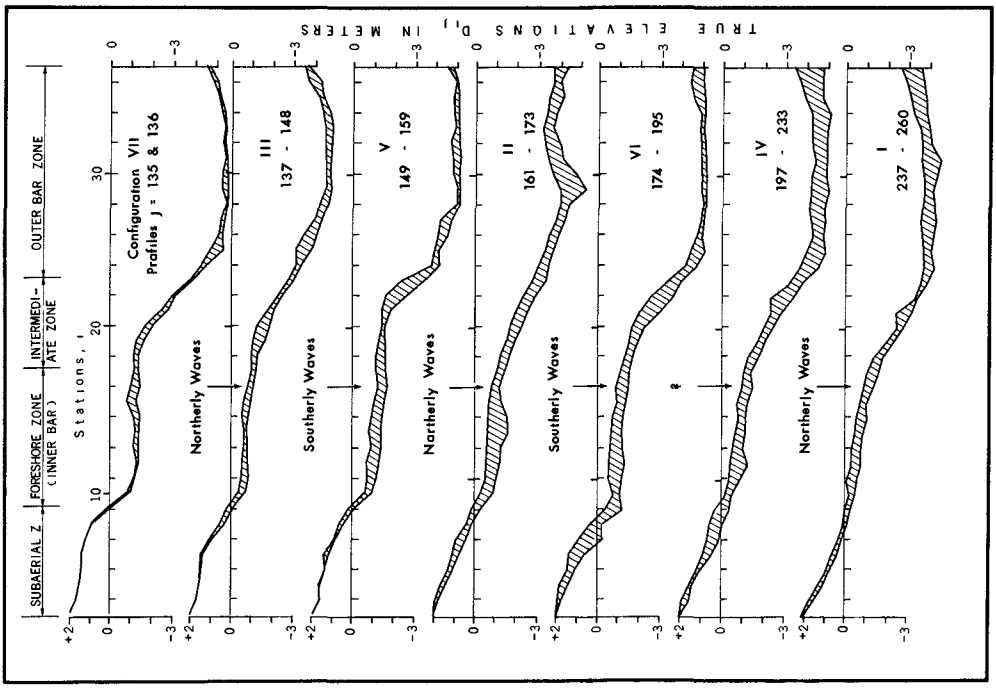

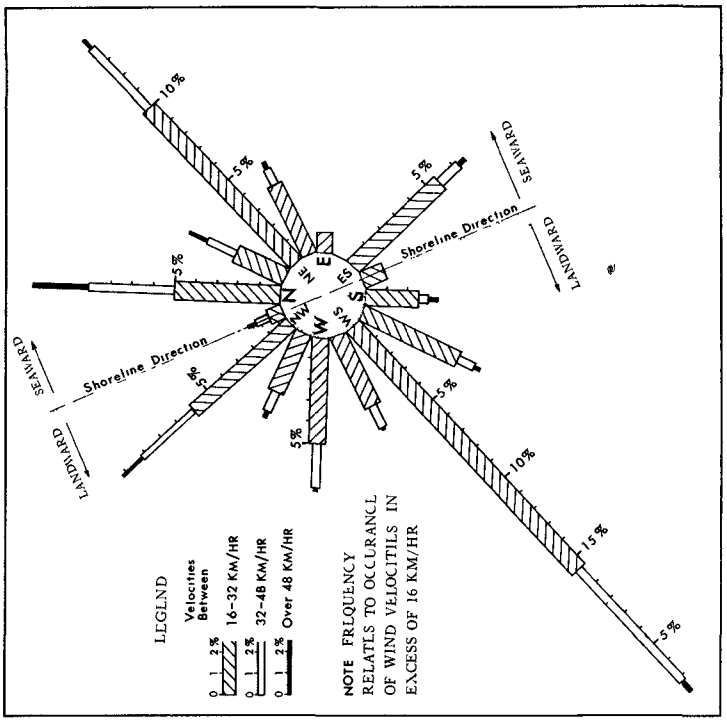

Fig. 8. Wind rose diagram from 2-hourly average velocities taken at Nags Head, Outer Banks, during observation of the 64 profiles analyzed here, January to March, 1964.

Fig. 9. Time history of profiles shown by true water depth $D_{i,j}$ below mean sea level. All 64 profiles are contained in these envelopes.

occurred: (1) profile change within each envelope, and (2) transition between envelopes.

Of particular interest is the influence of angle of wave incidence on profile responses. Changes within envelopes occurred when waves arrived normal to the shore and between envelopes during oblique wave incidence. Cut and fill suggested by changes in the fixed traverse were associated, respectively, to southerly and northerly wave incidences. In Figures 9 and 10, the transitions from envelopes III to V and from II to VI represent deepening associated with southerly waves, the transition from VII to III, from V to II, and from IV to I represent shoaling associated with northerly waves. From these observations it is inferred that profile change within an envelope results primarily from individual displacements of sediment along profiles, whereas the transition from one envelope to another results from profile displacements parallel to the shore. For sake of brevity, these two processes will be called transversal and alongshore responses.

RELATIONSHIPS WITH WAVE POWER

The physical criterion requires that energy influx be equivalent to the work produced. Consequently, certain relationships might be expected between the wave power and the capacity of the profile to accomodate it, and between the wave power and movement of material associated with the profile responses.

Airy's first-order approximation gives the wave power transmitted shoreward per unit width of wave crest by the following equation:

$$P = (\rho g H^2/8)\,(L/T) \cdot \tanh \frac{2\pi d}{L} \cdot n$$

in which ρ = specific gravity of sea water; g = gravity acceleration, H = wave height at depth d, L = wave length; T = wave period, and

$$n = 1/2[1 + (4\pi d/L)/(\sin 4\pi d/L)]$$

The profile capacity for accomodation can be represented by the sum of the water depths at all the stations within each profile, which is also an indicator of the general depth of this profile. Thus,

$$Y_j = \sum_{i=1}^{n} D_{i,j}$$

The relationships between P and Y_j are shown in Figure 11. The profile configurations are discriminated by different symbols and numbered in the increasing

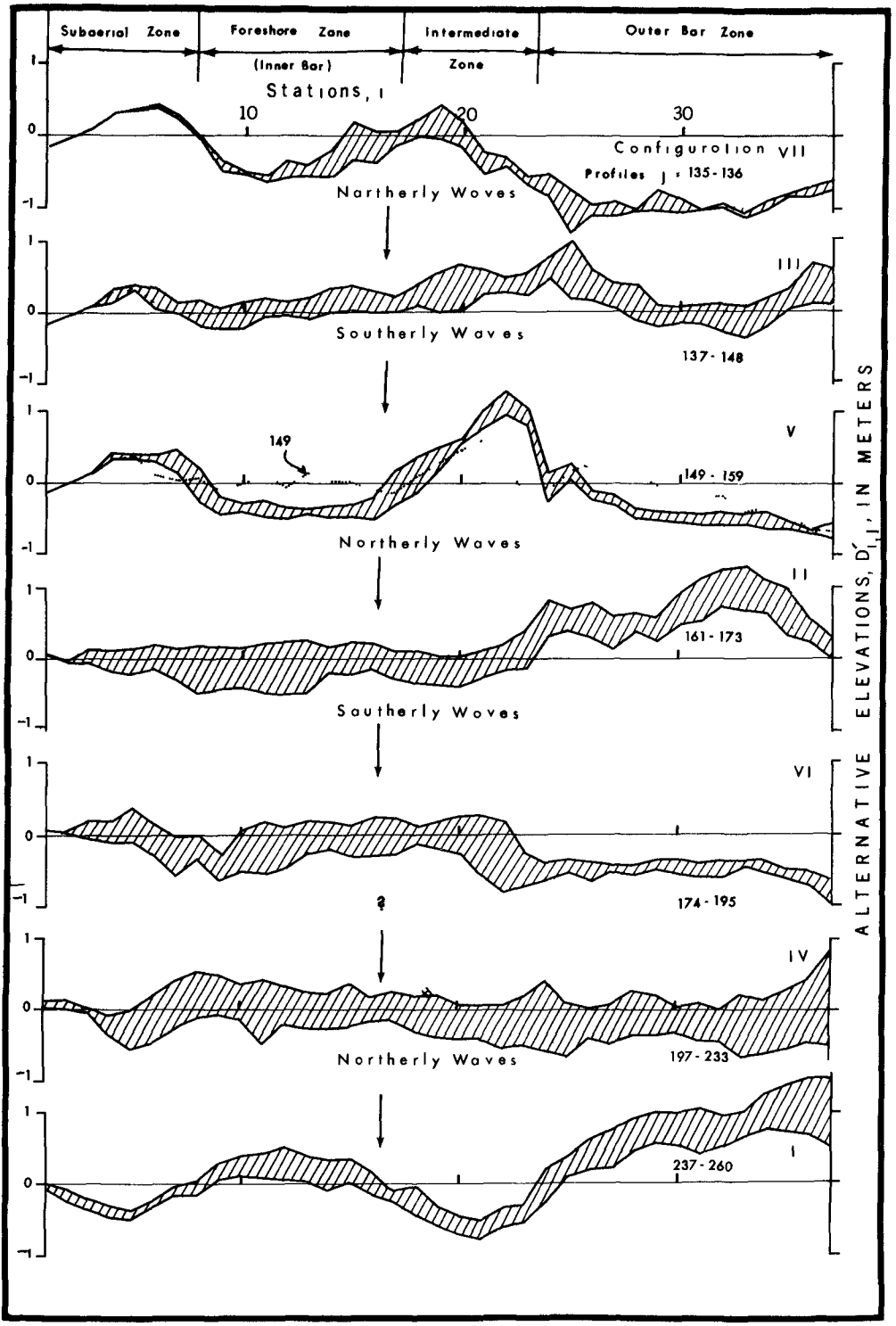

Fig. 10. Time history of profiles, shown by alternative depth: $D'_{I,J} = D_{I,J} - \bar{D}_I$. Envelopes

order of the general depths of profiles.

Two interesting relationships are implied: (1) In the transversal response - that is the changes within envelope – as the wave power increased, the depth of a profile also increased gradually, and (2) In the alongshore response – that is the changes from one envelope to another – the southerly waves caused deep profiles (shown by broken arrows) and the northerly waves shallow profiles (shown by solid arrows) at the traverse. In this case, as indicated by the coordinates of the arrows relative to the ordinate (wave power), the change was not influenced by the wave power but by whether the waves arrived from northerly or southerly quadrants.

Figure 12 shows the relationships between the wave power indicator (square of wave height) and the material movement involved in the 12-hour profile change. The latter term was computed by:

$$Q_j = \sum_{i=1}^{n} \left| D_{i,j+1} - D_{i,j} \right|$$

The plots were further discriminated by the following indicator to show whether or not the net material comprising the profile topography was preserved as a result of the profile responses, i.e.

$$Q'_j = \sum_{i=1}^{n} (D_{i,j+1} - D_{1,j}) \equiv \sum_{i=1}^{n} (\Delta D_{i,j})$$

in which n is the number of stations contained in the profile. Our data indicate that in 82 per cent of all the cases, the net material balance resulted in zero, i.e.

$$Q'_j \doteq 0$$

and in the remaining 18 per cent, in either erosion or accretion, i.e.

$$Q'_j \gtrless 0.$$

A further check with the wave data indicates that the former change was associated with perpendicular wave arrivals, while the latter with oblique wave arrivals. Thus, the transversal and the alongshore responses are again discriminated. The interpretation of Figure 12 is summarized as follows:

(1) In the transversal response - represented by blank plots - the scatter is small and indicates that the material moved in the traverse is proportional to

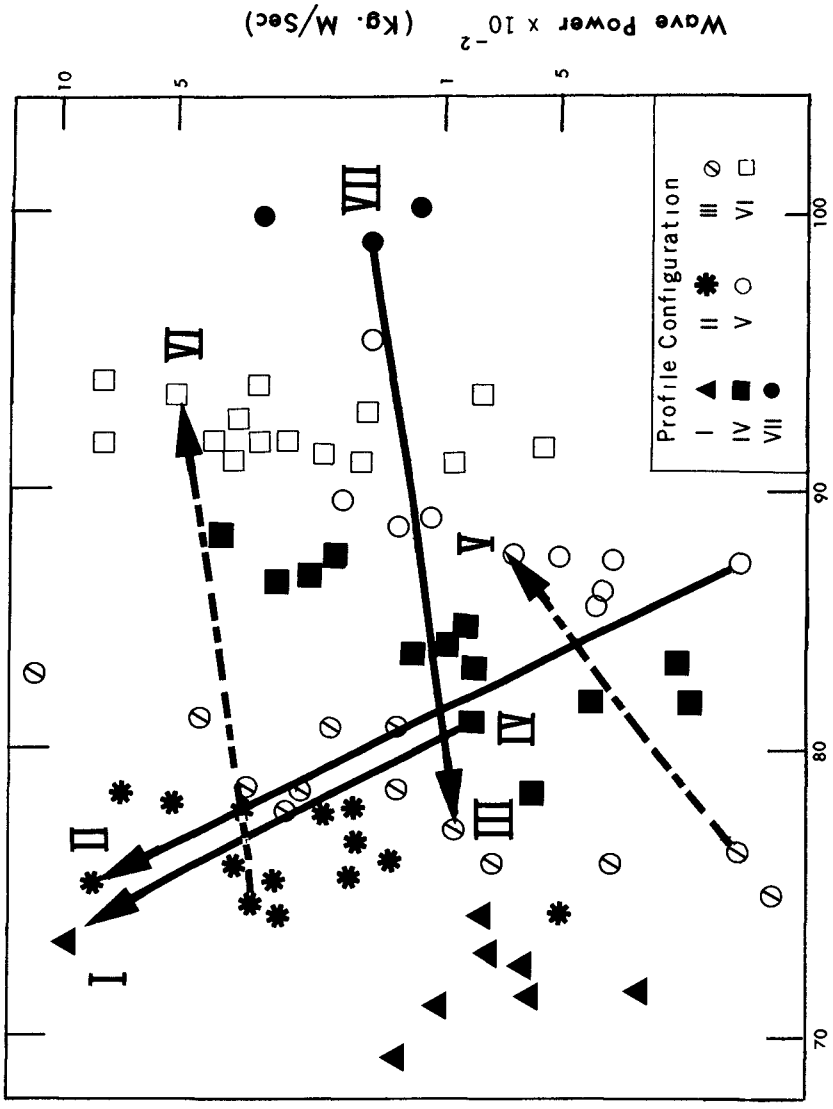

Fig. 11. Relationships between wave power, P, and general depth of profile, Y_j. Profiles discrimnated by general depths and shown by corresponding symbols (see inset).

the square root of wave height, namely,

$$Q_j = 2\ 1\ H^{\frac{1}{2}} \quad (H \text{ in meters})$$

(2) In the alongshore response – represented by the rest of the plots – the material moved in the traverse is several times greater than in the case of traversal response, and is not necessarily correlated with wave power. In other words, the profile change associated with alongshore response could take place with waves of very small power but arriving at oblique angles of incidence.

It is evident that these systematic relationships can be distinguished only by discriminating the plots on the basis of transversal and alongshore profile responses. Thus, the interpretation of Figure 12 can be extended further Let the wave power indicator H^2 be substituted by its transversal component, $H^2 \sin^2\Theta$, and plotted against the same indicator of material movement, Q_j, which is also the transversal component, so that a purely two-dimensional scheme may be simulated. However, since

$$H^2 >> H^2 \sin^2 \Theta$$

this procedure amounts to transposing the original plots for the alongshore response in Figure 12 toward the left side of the diagram, resulting in an even greater departure between the alongshore and the transversal responses. It then follows that contrary to a general belief, an interaction between wave and topography involving obliquely arriving waves may not simply be converted to a two-dimensional scheme by projecting wave variables onto a vertical plane perpendicular to the shore. By the same token, waves having an identical amount of transversal energy components but arriving at different angles of incidence, may not be expected to induce an equal amount of topographic response when (1) the observation is fixed at a stationary traverse and (2) the beach topography has a diversified contour system.

Figure 12 may be supplemented by simple statistics. Figure 13 shows histograms of 12-hourly elevation changes at individual stations for transversal and alongshore responses. The elementary term is expressed by

$$\Delta D_{i,j} = D_{i,j+1} - D_{i,j}$$

The histogram representing the transversal response resembles a normal distribution with the mean approximately at $\Delta D_{i,j} = 0$. This implies that in the transversal response the elevation changes at individual stations may be similar to a random fluctuation around the zero mean. The data representing the alongshore

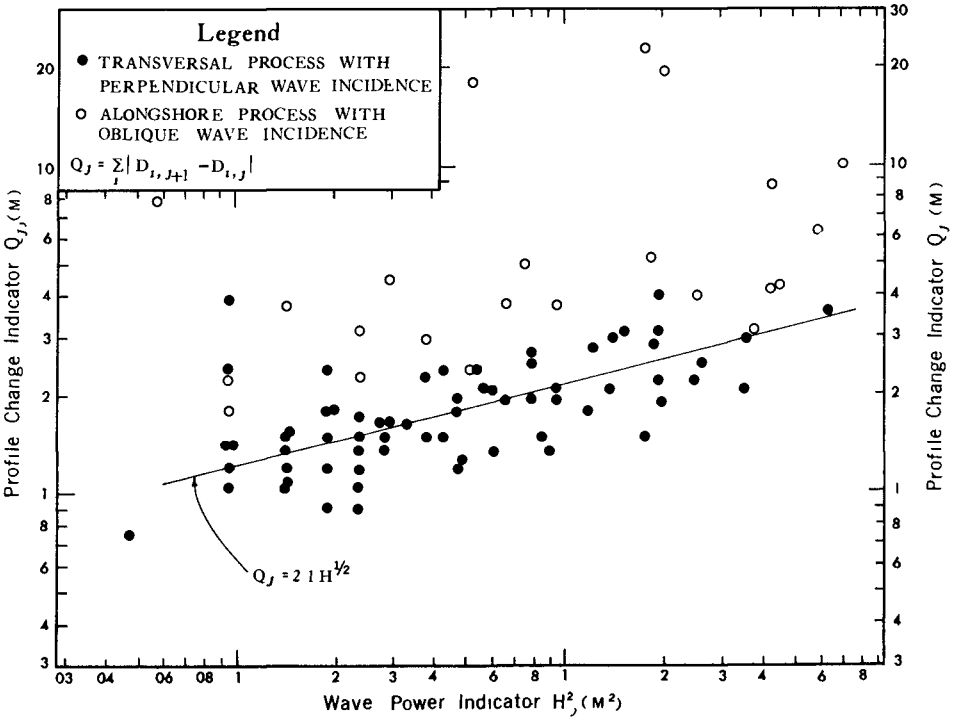

Fig. 12. Relationships between wave power indicator, H^2, and depth changes between 12-hourly consecutive profiles.

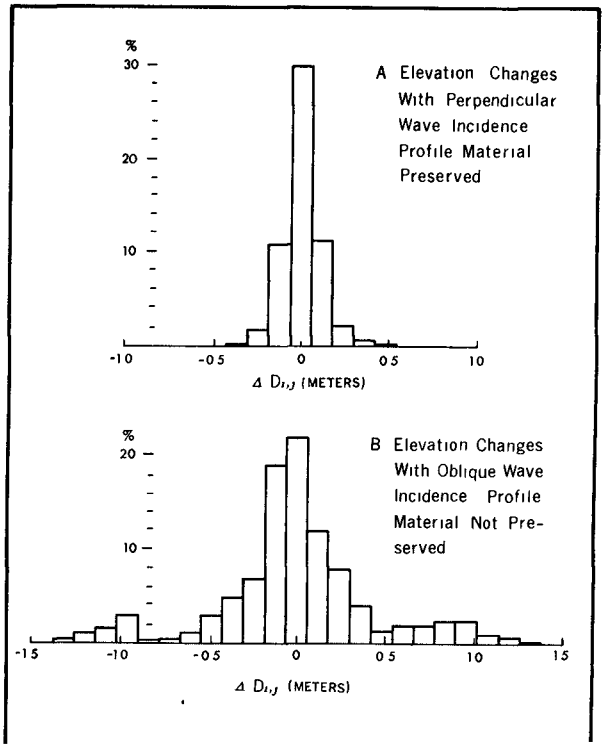

Fig. 13. Histograms of 12-hourly elevation changes combining all the stations of all the profiles.
A. Transversal response;
B. Alongshore response.

response result in a trimodal histogram, with the modes located approximately at $\Delta D_{1,j} = 0$ and ± 3.0 ft. Implications are that two alien processes are involved in this case. one similar to the preceding example of random fluctuation and the other involving an abrupt change of a larger order. Because of the extra modes, the standard deviation of $\Delta D_{i,j}$ in this case is nearly twice that of the preceding case, namely 1.13 ft/0.58 ft $\div$ 2/1

ZONAL CORRELATION WITHIN A PROFILE

The degree to which the change at a given station is related to the simultaneous change occurring at other stations in the profile can be expressed by the correlation coefficient as follows·

$$R_{1,k} = 1/N\text{-}1 \sum_{j=1}^{N-1} \frac{(\Delta D_{i,j} - \Delta \bar{D}_1)(\Delta D_k - \Delta \bar{D}_k)}{\sigma_1 \times \sigma_k}$$

$$\Delta \bar{D}_i = 1/N\text{-}1 \sum_{j=1}^{N-1} \Delta D_{1,j}$$

$$\sigma_1^2 = 1/N\text{-}1 \sum_{j=1}^{N-1} (\Delta D_{1,j} - \Delta \bar{D}_1)^2$$

i, k = 1, 2, ... n, station number, and
j = 1, 2, ... N, profile number.

The correlation coefficient, $R_{i,k}$, was computed for every pair of stations, and plotted in Figures 14 - A and B separately for the transversal and the alongshore processes of profile response. Again, a clear distinction is noted between the two processes. In the transversal response (Figure 14-A), the correlation level is generally low, and little or no pattern exists. However, in the alongshore response (Figure 14-B), a well definable pattern as well as the high level of correlation emerge. For instance, let us follow the correlation curve denoted by $R_{1,5}$, which represents the correlation between Station 5, located on the subaerial beach, and all other stations in the profile (Figure 14-B). Naturally, the correlation with itself is plus one, at Station 5, but this shifts to negative correlation with the stations of the foreshore (inner bar) zone, and then back to positive correlation with stations of the outer bar zone.

Accordingly, the surf-zone profile may be divided into four different segments - the subaerial zone (stations 1-7), the foreshore (inner bar) zone (stations 8-17), the intermediate zone (stations 18-23) and the outer bar zone (stations 24-37). It is then seen that in the case of alongshore response (Figure 14-B) the correlation is always negative between two adjacent zones and always positive between alternate zones. This feature appears to support the conventional notion regarding the transversal exchange of material in the beach profile, namely that material